

Direct regulation of abiotic responses by the Arabidopsis circadian clock component PRR7

Tiffany Liu, Jenny Carlsson^{†,‡}, Tomomi Takeuchi[†], Linsey Newton and Eva M. Farré*

Department of Plant Biology, Michigan State University, East Lansing, MI 48824, USA

Received 9 August 2012; revised 19 June 2013; accepted 24 June 2013; published online 28 June 2013.

*For correspondence (e-mail farre@msu.edu).

[†]Authors contributed equally to this work.

[‡]Present address: The Swedish Gene Technology Advisory Board, Retzius väg 13A, Solna, Sweden.

SUMMARY

Up to 30% of the plant transcriptome is circadian clock-regulated in different species; however, we still lack a good understanding of the mechanisms involved in these genome-wide oscillations in gene expression. Here, we show that PSEUDO-RESPONSE REGULATOR 7 (PRR7), a central component of the Arabidopsis clock, is directly involved in the repression of master regulators of plant growth, light signaling and stress responses. The expression levels of most PRR7 target genes peak around dawn, in an antiphasic manner to PRR7 protein levels, and were repressed by PRR7. These findings indicate that PRR7 is important for cyclic gene expression by repressing the transcription of morning-expressed genes. In particular we found an enrichment of the genes involved in abiotic stress responses, and in accordance we observed that PRR7 is involved in the oxidative stress response and the regulation of stomata conductance.

Keywords: circadian clock, *Arabidopsis thaliana*, pseudo-response regulator, ChIP-seq, stomata conductance, abscisic acid, oxidative stress.

INTRODUCTION

A diverse range of organisms have evolved time-keeping mechanisms, known as circadian clocks (Bell-Pedersen *et al.*, 2005). Circadian rhythms have an approximately 24-h period, persist under constant conditions, and are entrained by light and temperature. The ability to anticipate environmental change enables organisms to regulate biological processes in a timely order to optimize their growth and development (McClung, 2011). In the plant model organism *Arabidopsis thaliana*, the circadian clock regulates approximately 30% of the transcriptome (Covington *et al.*, 2008; Michael *et al.*, 2008), whereas about 90% of Arabidopsis genes display oscillations in expression levels under diel conditions (Michael *et al.*, 2008). Circadian clock-regulated transcription is involved in many plant processes, including metabolism, light signaling and floral development (Doherty and Kay, 2010). It also plays a key role in the regulation of stress responses, such as in response to cold, drought, oxidative stress and pathogen attack (Doherty and Kay, 2010; Lai *et al.*, 2012). Recent results show that the circadian clock-regulated expression of a significant number of genes is conserved across different plant species (Khan *et al.*, 2010; Filichkin *et al.*, 2011).

In the Arabidopsis circadian clock several components form interlocking feedback loops, which are a common feature of circadian clocks in eukaryotes (Bell-Pedersen *et al.*, 2005). Two homologous MYB transcription factors, CIRCADIAN CLOCK ASSOCIATED 1 (CCA1) and LATE ELONGATED HYPOCOTYL (LHY), peak close to dawn, and activate the expression of PSEUDO-RESPONSE REGULATOR 9 (PRR9) and PRR7 (Farre *et al.*, 2005). PRR9, PRR7 and PRR5 protein levels peak between the middle and the end of the day to repress CCA1 and LHY expression (Farre and Kay, 2007; Nakamichi *et al.*, 2010). In addition to activating gene expression, CCA1 and LHY repress the transcription of the evening-expressed genes TIMING OF CAB EXPRESSION 1/PSEUDO-RESPONSE REGULATOR 1 (TOC1/PRR1), EARLY FLOWERING 3 (ELF3), ELF4 and LUX ARRHYTHMO (LUX) (Nakamichi, 2011). In turn, these genes regulate the expression of CCA1 and LHY indirectly by repressing PRR9, PRR7 and/or PRR5 expression (Pruneda-Paz *et al.*, 2009; Dixon *et al.*, 2011; Gendron *et al.*, 2012; Huang *et al.*, 2012; Pokhilko *et al.*, 2012). In addition, TOC1 has also recently been shown to repress CCA1 and LHY expression directly (Gendron *et al.*, 2012; Huang *et al.*, 2012). Mutant analyses indicate that PRR9, PRR7 and PRR5 are

necessary for rhythmicity, and partly play overlapping roles in the regulation of both the circadian clock and clock output processes (Farre *et al.*, 2005; Nakamichi *et al.*, 2005, 2007, 2009, 2010). Circadian-regulated PRRs contain a pseudo-receiver domain, similar to the receiver domains of response regulators, and a CCT (CONSTANS, CONSTANS-like and TOC1) motif. The PRRs have been found to be associated with specific promoter regions *in vivo*, and are able to bind DNA *in vitro* (Pruneda-Paz *et al.*, 2009; Nakamichi *et al.*, 2010, 2012; Gendron *et al.*, 2012). For example, PRR9, PRR7, and PRR5 associate with the promoter regions of *CCA1* and *LHY* to repress their transcription (Nakamichi *et al.*, 2010). Mutations in any of these PRRs also result in alterations of numerous physiological and developmental processes, and these changes are exacerbated in higher order mutants. When compared with the wild type, the *prp5 prp7 prp9* triple mutant (*prp579*) is photoperiod insensitive and displays a very late flowering phenotype under long-day conditions (Nakamichi *et al.*, 2007). This triple mutant is also more drought and cold tolerant, and has perturbed metabolite levels, including an elevated abscisic acid (ABA) content (Fukushima *et al.*, 2009; Nakamichi *et al.*, 2009).

In order to understand the role of PRR7 in the regulation of plant growth and development, we identified genome-wide PRR7 targets in Arabidopsis by conducting chromatin immunoprecipitation combined with high-throughput sequencing (ChIP-Seq). Using this approach, we were able to identify 73 high-confidence PRR7 binding sites. Putative PRR7 target genes were enriched in morning-expressed circadian-regulated genes, and included master regulators of growth, light signaling and stress responses. In accordance, we found that PRR7 is involved in oxidative stress responses and regulation of stomata opening in Arabidopsis.

RESULTS

Identification of PRR7 target genes using ChIP-seq

Mutant expression analyses have shown that PRR7 influences numerous physiological processes in Arabidopsis. In order to identify the direct targets of PRR7 transcriptional regulation, we carried out two ChIP-Seq experiments using lines expressing HA-PRR7 under the control of its endogenous promoter that complement the long period circadian phenotype of *prp7-3* (*prp7*) (Farre and Kay, 2007). The ChIP-Seq data were analyzed using QUEST, a statistical package used to determine transcription factor binding sites (Valouev *et al.*, 2008; Appendix S1), and we identified 73 high-confidence binding sites in common between the two experiments (Appendix S1). Putative PRR7 target genes were defined as genes with binding sites located within 1000 bp upstream of a transcriptional start site to 1000 bp downstream of a transcriptional stop. Based on these

criteria, of the 73 HA-PRR7 specific binding sites, 17 did not associate with any annotated gene, whereas the remaining 56 associated with 83 genes (Appendix S1). Of these 83 putative PRR7 target genes, each gene associated with one binding site, except for *AT1G22767*, for which we identified two sites (Appendix S1). For 90% of the genes, the location of the PRR7 binding sites identified in experiments I and II differed by no more than 100 bp (Figure 1a). Our data confirmed the association of PRR7 with genomic regions close to the transcriptional start sites of *CCA1* and *LHY* (Figure S1a–d; Nakamichi *et al.*, 2010).

We further tested and confirmed the binding of PRR7 to 12 out of 19 binding sites identified in both experiments I and II in a PRR7-overexpressing line (*PRR7ox*) using three independent chromatin immunoprecipitation (ChIP) quantitative PCR assays (ChIP-qPCR) (Figure S1). Using this independent assay, we also tested and confirmed PRR7 binding to 20 out of 32 binding sites identified in one of the two ChIP-seq experiments (Appendix S1; Figure S1e,f). These target genes were selected based on their potential role in the phenotypes observed in *prp* mutants, and/or were members of gene families identified in the common set. Downstream analyses were performed on a total of 93 sites, composed of 73 identified in both ChIP-Seq experiments and the 20 sites that were independently confirmed. We will subsequently refer to these binding sites as PRR7 binding sites. These sites were associated with a total of 113 genes, which we will refer to as putative PRR7 targets (Appendix S1). The majority of PRR7 binding sites were located within 1000 bp upstream of a transcriptional start site, and 54% lie within 300 bp of a transcriptional start site (Figure 1b).

PRR7 represses the expression of target genes by binding to regions close to their transcriptional start sites

In order to study the effect of PRR7 on its target genes, we used publicly available data on gene expression in the *prp579* mutant (Nakamichi *et al.*, 2009) and analyzed RNA levels in *PRR7ox* (Farre and Kay, 2007) and *prp579* by reverse transcription-qPCR (RT-qPCR; Appendix S1; Figures 2, S2). We found an enrichment of genes upregulated in *prp579* among PRR7 targets (Fisher's exact test, $P < 0.0001$; Figure 1c). We observed a further enrichment of genes upregulated in *prp579* among genes that contain PRR7 binding sites upstream of their transcriptional start sites when compared with putative PRR7 targets with intragenic or downstream binding sites (Figure 1c; Fisher's exact test, $P < 0.05$). These results indicate that PRR7 associates with regions close to transcriptional start sites to repress transcription. Among the PRR7 binding sites, 16 are associated with the upstream region of one gene and the downstream region of another gene. In 64% of the cases analyzed (7/11), the gene with the PRR7 binding site closer to the transcriptional start site was upregulated in

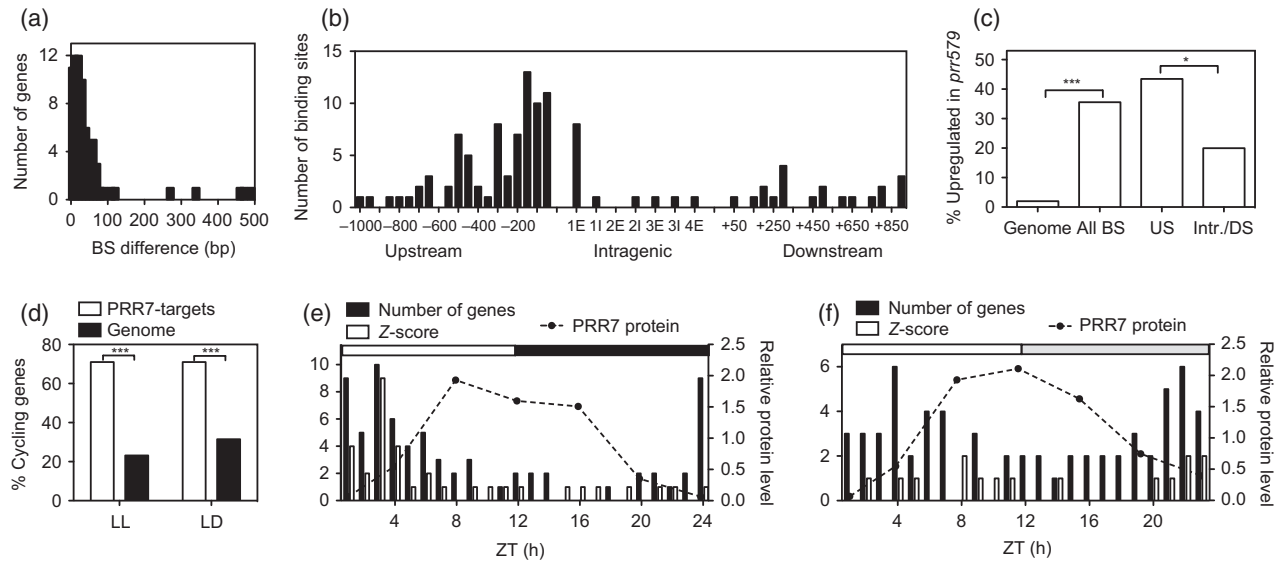


Figure 1. Location of PRR7 binding sites and expression patterns of putative PRR7 target genes.

(a) Differences in binding site location between experiment I and experiment II.

(b) PRR7 binding site locations in experiment II. These binding sites include sites in common between experiment I and experiment II, and the independently confirmed binding sites.

(c) Percentage of genes that display increased expression levels in the *prrr579* mutant.

(d) Percentage of genes with an upstream PRR7 binding site that display cycling expression levels. Data are taken from Edwards *et al.* (2006) for LL, and from Blasing *et al.* (2005) for LD. Cycling gene expression was analyzed using PHASER (Michael *et al.*, 2008). Genes were defined as cycling if model-based, pattern-matching algorithm > 0.8. The phase of cycling expression of genes associated with PRR7 binding sites under light/dark cycles (e) and under constant light conditions (f), as well as HA-PRR7 protein levels in *PRR7::HA-PRR7* expressing seedlings (from Farre and Kay, 2007).

Abbreviations: BS, binding site; DS, downstream (+1/+1000 from transcriptional stop); E, exon; I, intron; Intr., intragenic; LD, light/dark; LL, constant light; US, upstream (−1/−1000 from transcriptional start). Fisher's exact test: * $P < 0.05$; *** $P < 0.0001$.

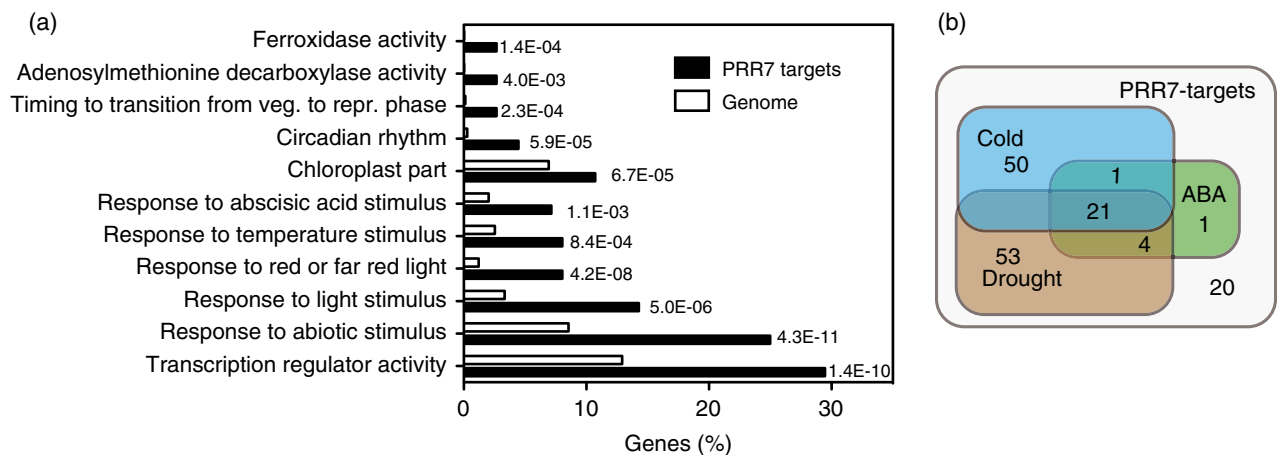


Figure 2. Analysis of putative PRR7 target genes.

(a) Enrichment of selected GO categories in PRR7 target genes. The numbers alongside the bars are P values for the EASE (Expression Analysis Systematic Explorer) score modified Fisher's exact test (Huang *et al.*, 2009a).

(b) Distribution of PRR7 targets among drought-, cold- and ABA-regulated genes.

prrr579 in the subjective evening, and downregulated in the *PRR7ox* line in the subjective morning (Figure S2a–h), suggesting repression by PRR7. We also identified a few genes with a PRR7 binding site in their downstream region displaying changes in expression in either the *prrr579* mutant

or the *PRR7ox* line (Figure S2a–c, e, g). As these genes show circadian oscillations, these effects might be caused indirectly by other clock components. In order to further study the role of the position of PRR7 binding sites on PRR7 regulation of gene expression, we identified PRR7

binding sites that were located upstream of the transcriptional start sites of two genes. In five of the six pairs analyzed, only one gene from each pair appeared to be repressed by PRR7 (Appendix S1; Figure S2i–k).

Of the PRR7 targets with an upstream binding site, 71% cycle under light/dark conditions, compared with 31% genome-wide (Fisher's exact test, $P < 0.0001$; Figure 1d; Michael *et al.*, 2008). In addition, 71% cycle under constant light conditions, compared with 23% genome-wide, revealing an enrichment in circadian-regulated genes among PRR7 targets (Fisher's exact test, $P < 0.0001$; Figure 1d; Michael *et al.*, 2008). Most of the PRR7 cycling target genes displayed a peak in expression between the end of the night and early morning under both light/dark cycles and constant light conditions (Figure 1e–f). This pattern of expression is antiphasic to PRR7 protein levels that peak at the end of the day (Farre and Kay, 2007), and agrees with the recent results showing that PRR7 can act as a transcriptional repressor (Nakamichi *et al.*, 2010). In general, PRR7 overexpression resulted in decreased peak RNA levels of PRR7 target genes, whereas the expression levels of PRR7 targets were elevated in the *prp579* mutant at the troughs, compared with the wild type (Figure S2). This pattern of changes in expression is similar to what occurs in overexpressing and mutant lines of other clock components that act as repressors, such as TOC1 (Huang *et al.*, 2012), CCA1 and LHY (Wang and Tobin, 1998; Mizoguchi *et al.*, 2002; Pruneda-Paz *et al.*, 2009), and ELF3, ELF4 and LUX (Dixon *et al.*, 2011; Nusinow *et al.*, 2011).

PRR7 regulates the expression of other clock components and regulators of developmental processes

Functional analysis of PRR7 target genes showed an enrichment in transcriptional regulators (Figure 2a). These transcriptional regulators include other clock components as well as factors involved in plant growth, development, light signaling and stress responses (Figure 3). In addition to CCA1 and LHY, we found that PRR7 associated with the promoter of *PRR9* (Appendix S1). The expression level of *PRR9* is strongly reduced in the *PRR7ox* (Figure 3). Moreover, the *prp579* triple mutant displays a long hypocotyl phenotype under several growth conditions (Kunihiro *et al.*, 2011). Consistent with this phenotype, PRR7 targets include *PHYTOCHROME INTERACTING FACTOR 4* (*PIF4*) and *PIF5* (Appendix S1). These two genes encode for bHLH transcription factors that promote hypocotyl growth in the dark, and integrate both the clock and light to regulate hypocotyl growth in a diurnal pattern (Nozue *et al.*, 2007; Nusinow *et al.*, 2011; Kinmonth-Schultz *et al.*, 2013). Thus, the long hypocotyls observed in the *prp579* mutant may be attributed to the derepression of both *PIF4* and *PIF5* by PRR7 (Figure 3). In addition, PRR7 also represses the expression of the myb-like transcription factors *REVEILLE 1* (*RVE1*), *RVE2* and *RVE7* (Appendix S1; Figure 3). These

proteins are involved in the regulation of processes downstream of the circadian clock such as hypocotyl growth and flowering (Kuno *et al.*, 2003; Zhang *et al.*, 2007; Rawat *et al.*, 2009), and their elevated expression in the *prp579* mutant could also contribute to its long hypocotyl phenotype (Figure 3). Under both short-day and long-day conditions, the *prp579* triple mutant exhibits an extremely late flowering phenotype, suggesting that the PRRs may play a role in the photoperiodic control of flowering time (Nakamichi *et al.*, 2007). Indeed, this mutant displays elevated transcript levels of *CYCLING DOF FACTORS* (*CDFs*), which are negative regulators of *CONSTANS* gene expression (Nakamichi *et al.*, 2007; Song *et al.*, 2011). We found that PRR7 targets include *CDF2* and *CDF5*, and that their expression is reduced in the *PRR7ox* and elevated in the *prp579* triple mutant (Figure 3).

Among PRR7 targets, we identified several genes involved in light signaling (Appendix S1; Figure 3). For example, the expression of both *LONG HYPOCOTYL 5* (*HY5*) and *HY5-HOMOLOG* (*HYH*) is elevated in the *prp579* triple mutant, although only *HYH* is repressed in the *PRR7ox* line (Figure 3). These proteins encode homologous bZIP transcription factors, shown to mediate light responses and promote photomorphogenesis (Chattopadhyay *et al.*, 1998; Holm *et al.*, 2002). In addition, we found that PRR7 represses *ATTENUATED FAR-RED RESPONSE* (*AFR*), an F-box protein involved in phyA light signaling (Harmon and Kay, 2003), as well as *SALT TOLERANCE* (*STO*) and *SALT TOLERANCE-HOMOLOGUE* (*STH*), which are B-box transcription factors involved in red light dependent hypocotyl elongation (Indorf *et al.*, 2007; Kumagai *et al.*, 2008; Figure 3). Moreover, light-regulated genes were enriched among PRR7 targets (Fisher's exact test, $P < 0.0001$; Appendix S2; Figure 4a; Nozue *et al.*, 2011). Accordingly, most PRR7 target genes contained a G-box motif in their promoter regions (Figure 4b). G-box elements are over-represented in light-regulated genes, and several proteins involved in light signaling are known to bind to these DNA elements (Chattopadhyay *et al.*, 1998; Hudson and Quail, 2003; Yadav *et al.*, 2005; Oh *et al.*, 2009). To look for potential *cis*-regulatory elements directly involved in PRR7 function, we searched for conserved motifs in regions ± 50 bp from the PRR7 upstream binding sites. Using the software packages MEME (Bailey *et al.*, 2006) and WEEDER (Pavesi *et al.*, 2004) we only found a G-box-containing motif enriched in regions close to PRR7 binding sites (Figure 4d). The analysis of regions ± 100 and ± 250 bp from the PRR7 upstream binding sites also identified a G-box-containing motif (Figure S3). These findings suggest that a G-box is involved in the regulation of gene expression by PRR7.

In order to identify potential co-regulators of PRR7 targets, we compared them with the genome-wide targets of transcriptional regulators involved in light signaling. We

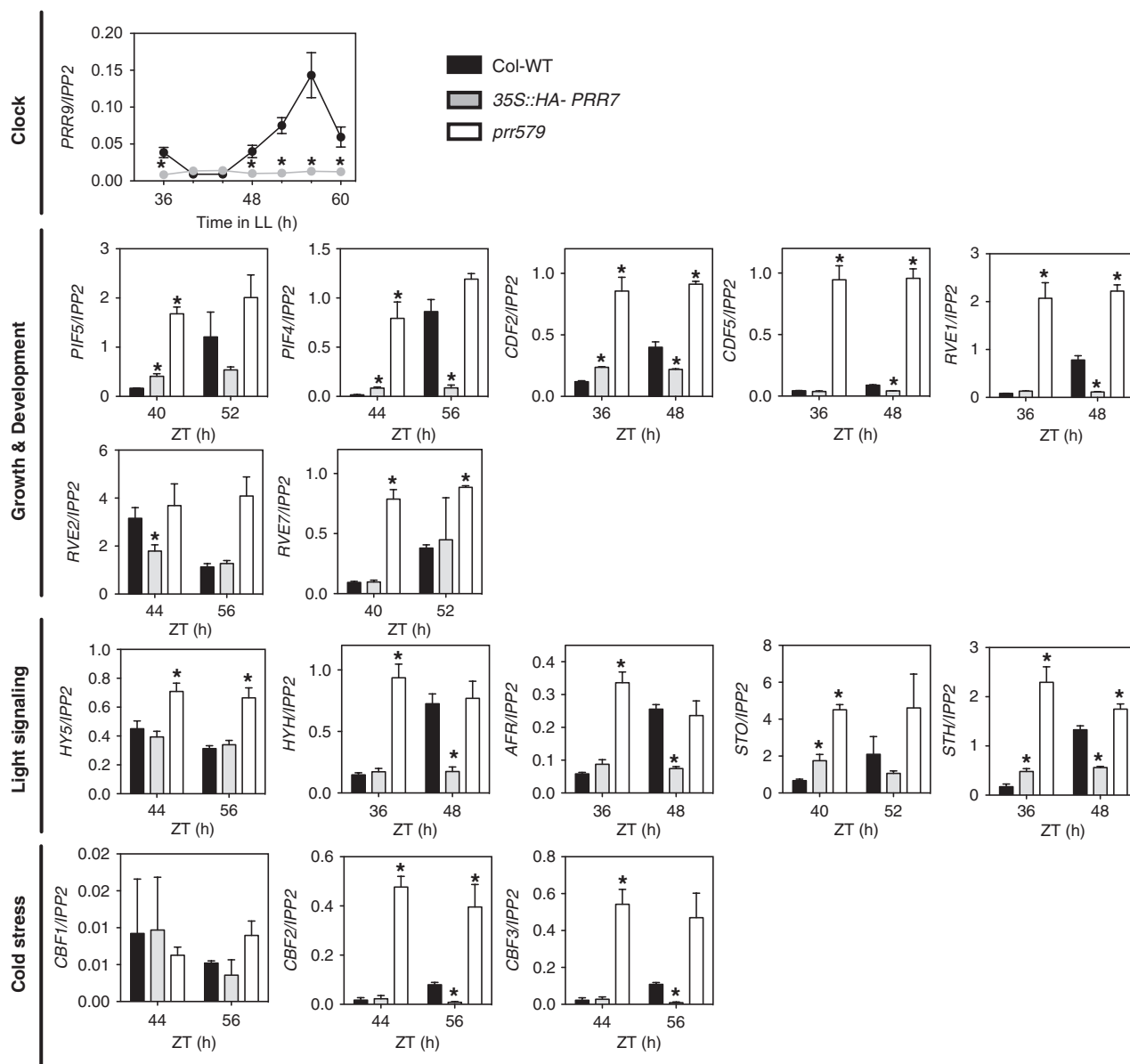


Figure 3. PRR7 directly regulates master regulators of the circadian clock, development and stress responses.

Expression analysis of these PRR7 target genes in the wild type (Col-WT), the PRR7 overexpressing line (35S::HA-PRR7) and the *prr579* triple mutant. Data are the averages \pm standard errors of two or three biological replicates. Expression level was analyzed by RT-qPCR and normalized to *IPP2*.

*Significant differences against the wild type (Student's *t*-test, $P < 0.05$).

found that a significant number of PRR7 targets are also regulated by the G-box binding factors PIF1/PIL5 and/or HY5, as well as FAR-RED ELONGATED HYPOCOTYL 3 (FHY3; Appendix S2; Figure 4c; Fisher's exact test, $P < 0.0001$; Lee *et al.*, 2007; Oh *et al.*, 2009; Ouyang *et al.*, 2011). These results could explain the enrichment of genes involved in red and far-red light responses among putative PRR7 target genes (Figure 2a), and indicate that they might be co-regulated by different light signaling components. Finally, PRR5 and TOC1 transcriptional targets have recently been described, and comparative analysis shows that their target

genes overlap significantly with the PRR7 targets identified in this study (Figure 4e; Fisher's exact test, $P < 0.0001$; Huang *et al.*, 2012; Nakamichi *et al.*, 2012).

PRR7 is involved in the regulation of cold-regulated gene expression

The *prr579* triple mutant has been shown to be more cold and drought stress tolerant than wild-type plants (Nakamichi *et al.*, 2009). Consistent with these findings, PRR7 targets include *C-REPEAT/DRE BINDING FACTOR 1* (*CBF1*), *CBF2* and *CBF3*, which are AP2 domain-containing

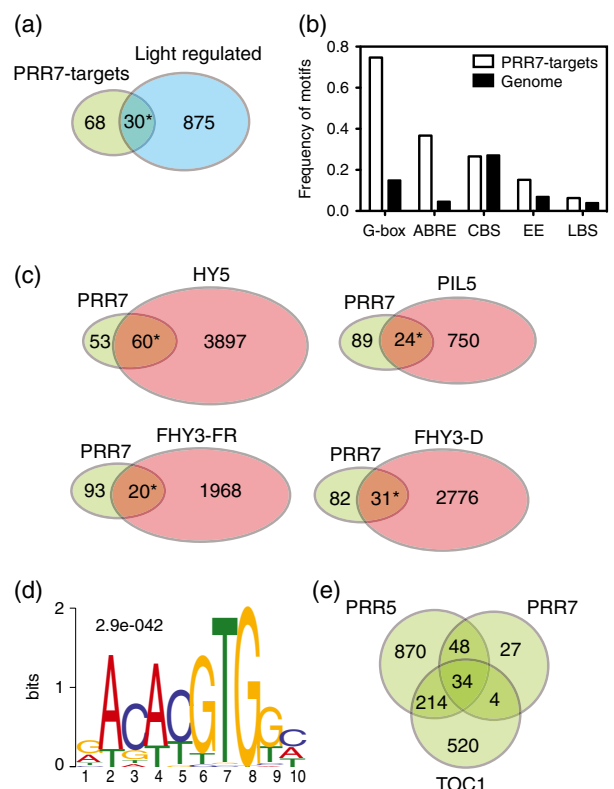


Figure 4. PRR7 target genes are light regulated.

(a) Venn diagram showing the overlap of PRR7 targets and light-regulated genes, as defined by Nozue *et al.* (2011).
 (b) Enrichment of known motifs in the upstream regions of PRR7 target genes.
 (c) Venn diagrams showing the overlap of PRR7 targets with HY5 (Lee *et al.*, 2007), PIL5 (Oh *et al.*, 2009) and FHY3 (Ouyang *et al.*, 2011) target genes. Abbreviations: ABRE, ABA-responsive element; CBS, CCA1 binding site; EE, evening element; LBS, LUX binding site; FR, far-red; D, dark.
 (d) A G-box motif was identified as the only statistically overrepresented motif in the 100 bp (50 bp on either side) regions surrounding PRR7 binding sites located upstream of a gene. Regions surrounding the PRR7 binding location from the common and independently confirmed binding sites were used as the input for MEME analysis.
 (e) Venn diagrams showing the overlap of PRR7 targets with PRR5 (Nakamichi *et al.*, 2012) and TOC1 target genes (Huang *et al.*, 2012). *Fisher's exact test, $P < 0.0001$.

transcriptional activators in the cold response pathway (Appendix S1; Gilmour *et al.*, 1998). The levels of *CBF2* and *CBF3* are constitutively upregulated in *prr579* and repressed in *PRR7ox* (Figure 3). The *prr579* triple mutant also displays constitutively higher induction of the three *CBFs* upon transfer to cold (Nakamichi *et al.*, 2009). Moreover, analyses of cold-stress microarrays (Kilian *et al.*, 2007) revealed that 73% of PRR7 targets are differentially regulated in response to cold, compared with 39% genome-wide (Fisher's exact test, $P < 0.0001$; Appendix S2). None of the PRR7 target genes are upregulated in *CBF*-overexpressing lines (Fowler and Thomashow, 2002). This indicates that the upregulation of cold-responsive

genes in the *prr579* mutant is not only caused by the effect of these pseudo-response regulators on *CBF* expression, but also suggests a wider role of the circadian clock in cold responses than previously thought (Dong *et al.*, 2011).

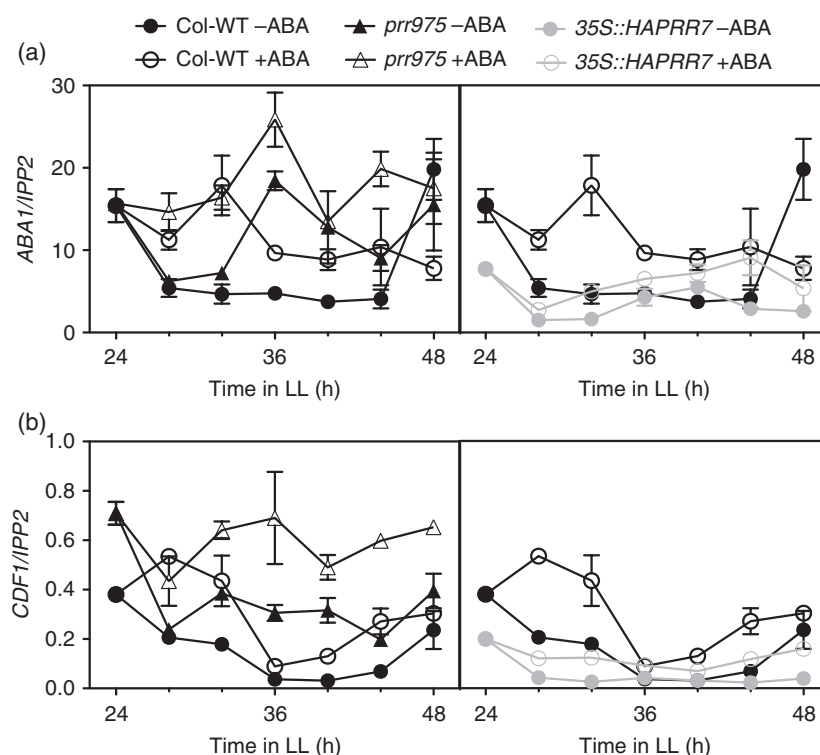
PRR7 regulates drought- and abscisic acid-responsive genes

We observed an enrichment in drought-responsive genes among the putative PRR7 targets, and found that 80% are drought responsive compared with 45% genome-wide (Fisher's exact test, $P < 0.0001$; Kilian *et al.*, 2007; Appendix S2). Furthermore, one PRR7 target is *ABA DEFICIENT 1* (*ABA1*; Appendix S1), which encodes a zeaxanthin epoxidase involved in ABA biosynthesis (Xiong *et al.*, 2002). The upregulation of *ABA1* (Figure 5) could explain the elevated levels of ABA observed in the *prr579* triple mutant (Fukushima *et al.*, 2009). In addition, general functional annotation analysis indicated an enrichment of ABA-regulated genes (Figure 2a), and we showed that 28% of PRR7 targets are regulated by ABA (Fisher's exact test, $P < 0.0001$) using data from Nemhauser *et al.* (2006; Appendix S2). Consistent with this finding, more than one-third of the PRR7 target genes contain ABA-responsive elements (ABREs) in their upstream regions (Figure 4b). The ABA-regulated genes comprise about half of the drought- and cold-responsive PRR7 targets (Figure 2b). Moreover, most of the PRR7 target genes that are drought responsive are also cold responsive and vice versa. These results suggest that PRR7 may regulate cold and drought responses in coordination with an ABA-dependent mechanism. We further investigated the role of PRR7 on ABA-regulated gene expression in PRR7 mutants and overexpressors. Genes induced by ABA, such as *CDF1* and *ABA1*, were less induced in the seedlings overexpressing PRR7 (Figure 5). We also investigated the physiological effects of PRR7 on ABA-regulated genes. The *prr579* mutants displayed a significant reduction in stomata conductance under well-watered conditions (Figure 6a). In order to test whether PRR7 could affect the plant sensitivity to ABA we analyzed the water loss of wild type and PRR7 misexpressing lines treated with this hormone. All plants including PRR7 overexpressors responded to the ABA treatment. ABA-treated overexpressors lost more water and the *prr579* mutant lost less water than ABA-treated wild-type plants after root detachment (Figure 6b). This suggests that factors other than ABA content affect water loss in PRR7-misexpressing plants.

It has been shown that ABA affects the period length of the circadian clock under constant light conditions (Hanano *et al.*, 2006). Therefore, we tested whether PRR7 could affect the sensitivity of the clock towards ABA. Under our experimental conditions, treatment with ABA led to a small reduction in the period length of wild-type seedlings, but to a stronger reduction in *prr7* mutants (Figure 7a–c). After

Figure 5. PRR7 modulates ABA-regulated gene expression.

Expression analysis of ABA regulated PRR7 target genes in the wild type (Col-WT), the PRR7 overexpressing line (*35S::HA-PRR7*) and the *prp579* triple mutant in the presence of ABA. Seedlings were treated with 10 μ M ABA at ZT0. Data are averages \pm standard errors of two or three biological replicates. The expression level was analyzed by RT-qPCR and normalized to *IPP2*.



treatment with exogenous ABA, the *prp7* mutants developed a shorter period than the wild-type plants (Figure 7c). The *prp57* and *prp79* double mutants also displayed a small reduction in period length after the addition of ABA. In contrast to the effects of ABA on *TOC1* (Legnaioli *et al.*, 2009; Figure S4), we did not observe any effect of exogenous ABA on *PRR7* gene expression (Figure 7d); however, the expression of *PRR7* was reduced in the ABA-deficient *npq2-1* mutant (Figure 7d).

PRR7 is involved in the adaptation to iron excess

PRR7 targets also included three *FERRITINS*: *FER1*, *FER3* and *FER4*. These genes are some of the few PRR7 targets for which expression peaks in the evening in wild-type seedlings (Figure 8). The RNA levels of *FER1*, *FER3* and *FER4* are reduced in *PRR7ox*, whereas their expression is elevated during the subjective day in the *prp579* mutant (Figure 8). Ferritins have been proposed to protect plants against oxidative stress caused by excess iron (Briat *et al.*, 2010), and the *fer134* triple mutant displays increased sensitivity towards excess iron when grown on soil (Ravet *et al.*, 2009). Therefore, we tested whether the misexpression of PRR7 would lead to a defect in the adaptation to iron excess media. PRR7 overexpressing lines were more sensitive to iron excess and displayed a significant reduction in chlorophyll content when grown under high iron conditions (Figure 9a). In contrast, higher order *prp* mutants appeared almost insensitive to the addition of iron (Figure 9a). Under the conditions tested, the *fer134* mutant

did not display an increased sensitivity towards excess iron, indicating that other mechanisms mediate the role of PRRs in oxidative stress (Figure 9b). It has recently been shown that *CCA1* and *LHY* regulate the levels of reactive oxygen species (Lai *et al.*, 2012). As PRR7 represses the expression of *CCA1* and *LHY* (Farre and Kay, 2007; Nakamichi *et al.*, 2010; #402), we analyzed the sensitivity of the *cca1lhy* mutant and the *CCA1ox* line to excess iron. In agreement with the role of *CCA1* and *LHY* in protecting against reactive oxygen species, the *cca1lhy* mutant was significantly more sensitive to iron excess than the wild type (Figure 9c). We therefore assessed the iron sensitivity of *prp79* mutants with reduced levels of *CCA1* and *LHY* (Salome and McClung, 2005). In spite of their decrease in *CCA1* and *LHY* expression (Figure S5), these lines still displayed a decreased sensitivity to iron excess (Figure 9d), suggesting an independent role of PRRs under oxidative stress.

DISCUSSION

PRR7 is a repressor of gene expression

Our results suggest that PRR7 represses gene expression by binding to regions close to transcriptional start sites. We did not find any evidence for PRR7 acting as a transcriptional activator. These findings suggest that the mechanism of transcriptional regulation by PRR7 could be the same for all of its target genes. PRR5, PRR7 and PRR9 contain a partially conserved amino acid sequence shown

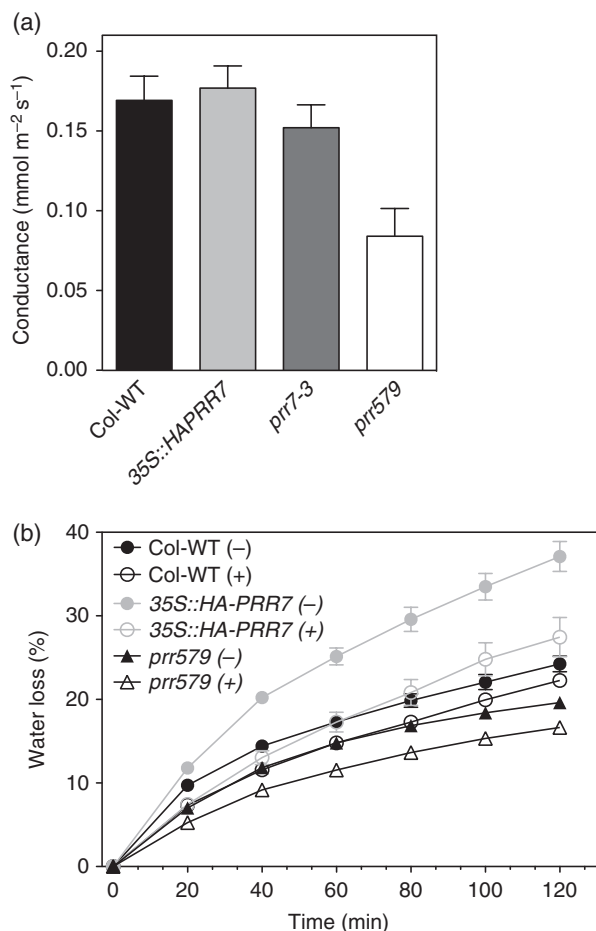


Figure 6. PRR7 affects leaf stomata conductance. (a) Stomata conductance of 7-week-old plants. Data represent averages \pm standard errors of between four and six plants. (b) Rates of water loss of detached rosettes. Plants were treated with either 10 μ M ABA in water (+) or water with methanol (–), as a control, at ZT1. Three hours later at ZT4.5 rosettes were detached and the weight loss was measured over a 2-h period. Data represent means \pm standard errors of five rosettes per genotype and treatment. Both experiments were performed twice with similar results.

to be necessary for repressing transcription in yeast (Nakamichi *et al.*, 2010). This conserved EAR (ethylene-responsive element binding factor-associated amphiphilic repression) motif is located in the variable domain of these PRRs, between the highly conserved pseudo-receiver and CCT domains. It has recently been shown that PRR5, PRR7 and PRR9 associate with the plant Groucho/Tup1 co-repressor family, TOPLESS/TOPLESS-RELATED, via the EAR motif, to repress the transcription of *CCA1* and *LHY* (Wang *et al.*, 2013). The CCT domain shares some sequence similarity with the DNA binding domain of yeast HEME ACTIVATOR PROTEIN 2 (HAP2), which is a subunit of the HAP2-HAP3-HAP5 trimeric complex that binds to CCAAT boxes in eukaryotic promoters (Wenkel *et al.*, 2006). The CCT domain of PRR5 is necessary for

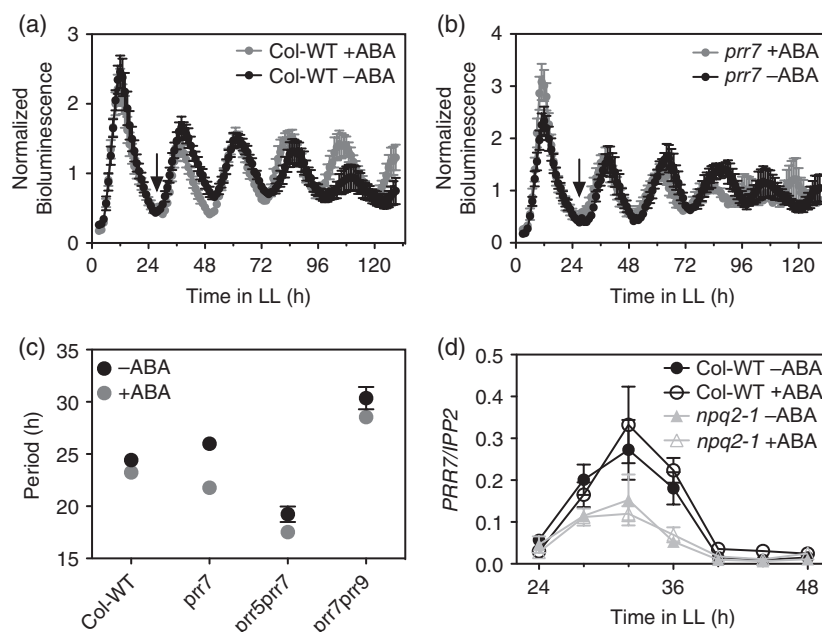
association with DNA *in vivo* (Nakamichi *et al.*, 2012), and the CCT domain of several circadian clock-regulated PRRs, including PRR7, has also been shown to bind DNA directly *in vitro* (Gendron *et al.*, 2012). However, the DNA-binding specificity of the PRRs remains unknown. The transcriptional regulation activity of the PRRs might also be mediated by their interaction with DNA-binding transcriptional regulators. For example, TOC1 has been shown to interact with CHE1 and several bHLH transcription factors (Yamashino *et al.*, 2003; Kidokoro *et al.*, 2009; Pruneda-Paz *et al.*, 2009). Our results indicate that a G-box motif is enriched in regions very close to the PRR7 binding sites. This finding suggests that PRR7 could mediate regulation directly or through G-box binding proteins. The G-box is also enriched in regions close to PRR5 and TOC1 binding sites (Huang *et al.*, 2012; Nakamichi *et al.*, 2012), indicating that these three pseudo-response regulators might be binding to the same promoter regions. Moreover, G-box-like promoter elements mediate light and ABA signaling processes (Jiao *et al.*, 2007; Cutler *et al.*, 2010). The combinatorial effect of PRR7 and these signaling pathways are likely to cause the differences in the phase of expression of PRR7 target genes between constant light and light/dark cycles (Figure 1e,f).

PRR7 represses the expression of other clock proteins and master regulators of plant growth, development and response to abiotic stress

Other clock genes were identified among the strongest bound targets in our experiments. We found that PRR7 directly regulates morning-expressed *PRR9*, in addition to *CCA1* and *LHY*. Similar experiments on the mammalian clock component BMAL1 have also shown stronger binding to other clock components than to clock output genes (Rey *et al.*, 2011). These differences in binding could reflect differences in tissue-specific expression, tissue-specific association and/or overall binding affinity. Among PRR7 targets, we found a significant enrichment of transcription factors. The presence of a large number of transcription factors among first-order circadian clock-regulated genes indicates that the circadian clock regulates output processes in a hierarchical fashion. However, as has been shown for BMAL1 in mice (Rey *et al.*, 2011), PRR7 also regulates a significant number of non-regulator targets. The identified direct targets of PRR7 can explain most of the observed phenotypes of the *prr579* triple mutant, such as cold and drought tolerance, long hypocotyl and late flowering. As PRR5 and PRR9 are also able to directly regulate the expression of *CCA1* and *LHY*, it was expected that their target promoters would also overlap significantly with PRR7 targets. PRR5 transcriptional targets have recently been identified using a ChIP-seq approach, and they include a significant number of genes also regulated by PRR7. Among these common targets are key transcription

Figure 7. ABA affects the period length of *prp7* mutants under constant light conditions. *CCR2::LUC* bioluminescence rhythms in wild type (a) or *prp7* mutants (b) in the presence or absence of exogenous ABA.

(c) Period length estimates of the *CCR2::LUC* bioluminescence rhythms shown in (a) and (b), and in the *prp57* and *prp79* double mutants. (d) *PRR7* RNA levels in the presence or absence of exogenous ABA. Seedlings were treated with 10 μ M ABA at ZT0. Data are averages \pm standard errors of three biological replicates. The expression level was analyzed by RT-qPCR and normalized to *IPP2*.



factors, such as *RVE1* and *RVE7*, *CDF2* and *CDF5*, *PIF4* and *PIF5*, and *CBF1/2/3*. Interestingly, *PRR7* and *PRR5* also share a large number of target genes with *TOC1* (Figure 4e). Most of *PRR5*-, *PRR7*- and *TOC1*-regulated genes peak in the morning in an antiphasic manner to the late-day/dusk expression of these proteins. The consecutive expression of *PRR7*, *PRR5* and *TOC1* therefore leads to the repression of their targets during a wide window between late day and early night.

PRR7 modulates ABA-regulated gene expression

A significant number of *PRR7* target genes are regulated by ABA, and we observed that changes in *PRR7* levels influence the response of these genes to the hormone (Figure 5). Interestingly, even under the exogenous application of ABA, the expression of *CDF1* cycles in wild-type seedlings under constant light conditions, with little or no activation observed at dusk (Figure 5), which coincides with the peak of *PRR7* protein levels. Our analysis of *PRR7* mutants and overexpressors indicate that *PRR7* is at least partly responsible for that time-dependent response to ABA. In spite of the effects of *PRR7* on ABA-mediated expression changes, *PRR7* mutants and overexpressors still responded to the ABA promotion of stomata closing (Figure 6b). Moreover, *PRR7* is associated with the upstream regions of several genes involved in ABA signaling, such as *HY5* (Chen *et al.*, 2008), *GENOMES UNCOUPLED 5* (*GUN5*; Du *et al.*, 2012) and *ABI FIVE BINDING PROTEIN 4* (*AFP4*; Garcia *et al.*, 2008). *GUN5* is also directly repressed by *TOC1*, and *TOC1* overexpressors display changes in ABA sensitivity in stomata closing. A possible explanation for this difference in response to ABA between *TOC1* and *PRR7* misexpressing lines might result

from differences in tissue-specific expression among the *PRRs*. Although *PRR5*, *PRR7*, *PRR9* and *TOC1* are expressed in the phloem, only *TOC1* is significantly expressed in the stomata (Figure S6; Mustroph *et al.*, 2009). Finally, we observed that *prp7* mutant period length was more sensitive to exogenous ABA than the wild type (Figure 7a–c). ABA affects *TOC1* expression (Huang *et al.*, 2012; Legnaioli *et al.*, 2009; Figure S4) but not *PRR7* RNA levels (Figure 7d) under constant light conditions, and therefore the mechanism behind this difference in ABA sensitivity of the *prp7* mutants remains to be studied.

PRR7 mediates sensitivity against oxidative stress

PRR7 overexpressors and *prp579* triple mutants displayed changes in sensitivity to oxidative stress caused by excess iron. Our results indicate that this is not caused solely by the role of *PRRs* on *CCA1* and *LHY* expression, which have recently been shown to play a direct role in the time-dependent protection against reactive oxygen species (Lai *et al.*, 2012). In addition to three ferritin genes that have been shown to be involved in the protection against excess iron (Ravet *et al.*, 2009), *PRR7* targets also include a superoxide dismutase family protein (At3g56350). It has been shown that the overexpression of Arabidopsis *CBF1* in transgenic *Solanum lycopersicum* (tomato) also leads to an increased tolerance against oxidative damage (Hsieh *et al.*, 2002). Therefore, the strong changes in *CBF1*, *CBF2* and *CBF3* expression in *PRR7* mutants and overexpressors could also be partly responsible for these changes in sensitivity to oxidative stress.

In conclusion, our studies show that *PRR7* directly regulates a significant number of genes involved in the response to abiotic stimuli. Most *PRR7* targets are

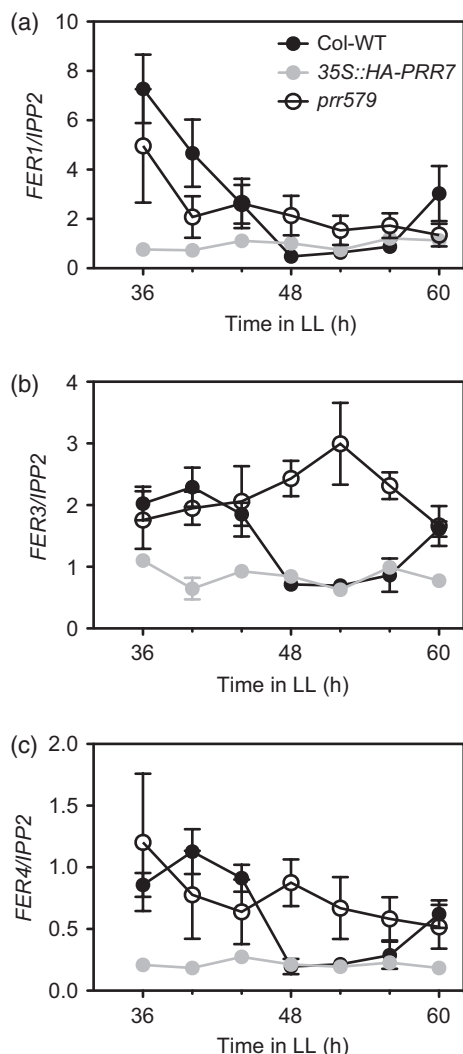


Figure 8. PRR7 directly regulates ferritin gene expression. RNA levels of *FER1* (a), *FER3* (b) and *FER4* (c) in the wild type (Col-WT), the PRR7 overexpressing line (35S::HA-PRR7) and the *prr579* triple mutant. Data are averages \pm standard errors of two or three biological replicates. The expression level was analyzed by RT-qPCR and normalized to *IPP2*.

expressed in the morning and are co-regulated by light, drought and/or cold signaling pathways, as well as by other clock components. Taken together, these results establish the role of clock components directly regulating multiple signaling pathways in a time-dependent manner.

EXPERIMENTAL PROCEDURES

Plant materials

The Arabidopsis lines *prr7-3*, *prr9-1*, *prr79* (*prr7-3 prr9-1*), *prr79 CCR2::LUC* (Farre et al., 2005), *prr7-3 PRR7::HA-PRR7* #151 (Farre and Kay, 2007), 35S::HA-PRR7 #54 (Farre and Kay, 2007), 35S::PRR7 #5 (Farre and Kay, 2007), *CCA1ox* (35S::CCA1 #34) (Wang and Tobin, 1998), *cca1lhy* (*cca1-11 lhy-21* CS9380; Dong et al., 2011), *npq2-1* (Niyogi et al., 1998), *fer123* (Ravet et al., 2009)

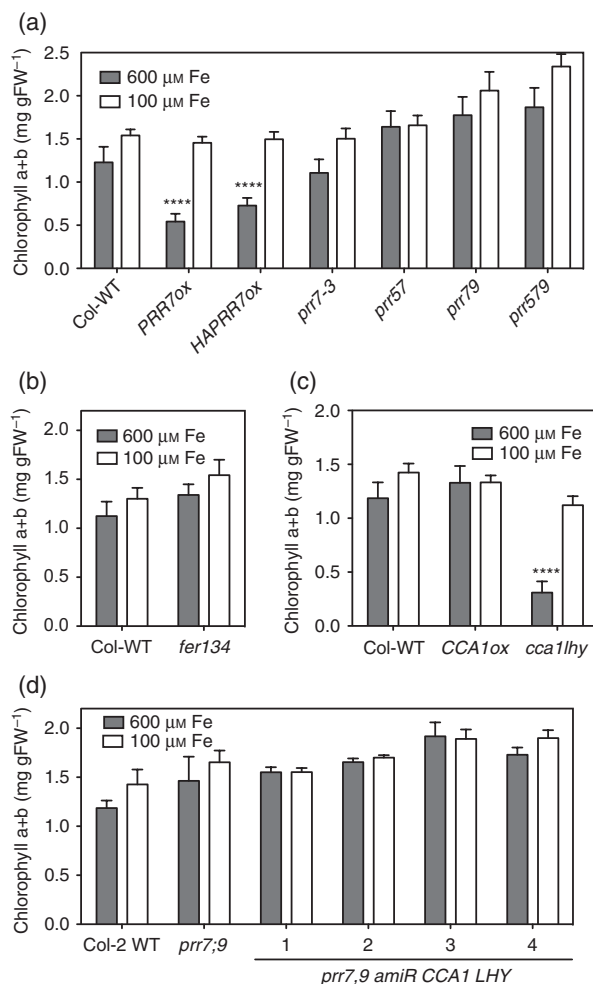


Figure 9. PRR7 affects sensitivity to iron excess. Seedlings were grown for 3 weeks in MS without sucrose media (100 μ M iron) before being transferred to MS without sucrose media supplemented with 500 μ M iron EDTA (total iron concentration of 600 μ M) for 4–7 days before the analysis of chlorophyll content. FW, fresh weight. Data represent averages \pm standard errors of between four and 12 biological replicates from two or three independent experiments. ****Significant differences against 100 μ M Fe (Student's *t*-test, *P* < 0.0001).

were previously described. The lines *prr7 prr9* (*prr7;9*) and *prr7;9 amiR-CCA1-LHY* are in the Col-2 *CCA1::LUC* background (Salome and McClung, 2005). The lines *prr57* (*prr5-1 prr7-3*) and *prr579* (*prr5-1 prr7-3 prr9-1*) were generated by crossing. *prr57 CCR2::LUC* was generated by transformation (Strayer et al., 2000).

Growth conditions

For gene expression and ChIP experiments, seedlings were grown on MS medium (Murashige and Skoog, 1962) with 0.8% agar and 2% sucrose under 70 μ mol m⁻² sec⁻¹ and a 12-h light/12-h dark regime at 22°C for 2 weeks. For the analysis of ABA-regulated gene expression, plants were treated with 10 μ M ABA or ethanol control in 0.01% silwett at ZT24, and transferred to constant light. For the iron excess experiments sterilized seeds were germinated on plates containing (MS) medium without sucrose, and were grown for 3 weeks under a 70 μ mol m⁻² sec⁻¹ and a 12-h

light/12-h dark regime. The seedlings were then transferred to a new MS media plate (100 μM iron), or MS medium supplemented with iron EDTA to achieve a final iron concentration of 600 μM . The plates were moved to constant light (70 $\mu\text{mol m}^{-2} \text{sec}^{-1}$) the next day at Zeitgeber time 0 (ZT0), and were kept in constant light for 4–7 days before the analysis of chlorophyll content. For stomata conductance, seeds were sown on soil in Ray Leach 'Cone-tainers' (Stuewe & Sons, Tangent, OR, USA). After a 3-day imbibition at 4°C, the wild type, *prp7* mutant and PRR7 overexpressors were grown under 120 $\mu\text{mol m}^{-2} \text{sec}^{-1}$, 8-h light/16-h dark, short days, at 24°C light/20°C dark, for 7 weeks until the gas-exchange experiments were performed. For the *prp579* triple mutant, the plants were grown under 120 $\mu\text{mol m}^{-2} \text{sec}^{-1}$, 16-h light/8-h dark, long days, at 24°C light/20°C dark, for 6 weeks, and the plants were transferred to an aforementioned short-day regime 10 days before the gas-exchange measurements were performed. The rosette leaves of the triple mutant remained too small for single-leaf conductance analysis under short-day growth conditions. For the water loss assays, 4-week-old plants grown on soil under 100 $\mu\text{mol m}^{-2} \text{sec}^{-1}$, 16-h light/8-h dark, at 22°C, were treated with either 10 μM ABA in water or water with methanol as the control at ZT1. Three hours later at ZT4.5, rosettes were detached and the weight loss was measured over a 2-h period.

Chromatin immunoprecipitation, library preparation and sequencing

Chromatin immunoprecipitation was carried out by a modified protocol based on the method described by Sawa *et al.* (2007). Details are described in Appendix S4. Arabidopsis seedlings were harvested at ZT12. For each ChIP we used approximately 120 μg of DNA. The protocol for library preparation for sequencing is described in the Appendix S5. For each library, we pooled five (experiment I) and 12 (experiment II) individual immunoprecipitated DNA and respective input DNA using the QIAquick® PCR Purification Kit (Qiagen, <http://www.qiagen.com>). Adapter sequences are described in Appendix S3. The DNA size and quality was controlled using the BioAnalyser DNA high sensitivity kit (Agilent, <http://www.agilent.com>) and Fluorometer Qubit (Invitrogen, <http://www.invitrogen.com>). Single-end Illumina sequencing by synthesis was performed by the Michigan State University Research Technology Support Facility.

Analysis of the enrichment of immunoprecipitated DNA by quantitative PCR

A 1.5- μl aliquot of DNA was used for PCR amplification by qPCR using an Eppendorf single-color real-time PCR detection system (Master Cycle Realplex2; <http://www.eppendorf.com>). Two technical replicates were analyzed for each sample. Quantification was carried out by PCR base line subtracted curve fit with the provided REALPLEX software. Primers are described in Appendix S3. The intron of *ACT2* (AT5G09810) was used as a negative control. Details on the use of different HA-PRR7 expressing lines are described in Appendix S6.

Expression analysis by RT-qPCR

RNA was extracted using the Plant RNA Kit according to the manufacturer's recommendations (Omega, <http://www.omegachemical.com>). The iScript cDNA synthesis kit (Bio-Rad, <http://www.bio-rad.com>) was used for reverse transcriptase-mediated PCR. The cDNA was diluted five times with water, and 1.5 μl was used for PCR amplification by real-time PCR as described for the detection of immunoprecipitated DNA. Two technical replicates were analyzed

for each sample. Primers are described in Appendix S3. The gene *IPP2* (AT3G02780) was used as a normalization control.

ChIP-Seq data analysis

Sequences were preprocessed using the FASTX toolkit (http://hannonlab.cshl.edu/fastx_toolkit) and aligned to the Arabidopsis TAIR10 genome using BOWTIE (Langmead *et al.*, 2009). QUEST (Valouev *et al.*, 2008) was used to identify binding sites and determine false discovery rates (FDRs). In experiment I, each immunoprecipitated sample from *prp7-3 PRR7::HA-PRR7* and *prp7-3* were compared with their respective inputs as negative controls. After discarding 11 binding sites common between the two sets, we identified 674 sites specific to *prp7-3 PRR7::HA-PRR7*. In experiment II, we compared the immunoprecipitated *prp7-3 PRR7::HA-PRR7* with the immunoprecipitated *prp7-3* as a negative control, and identified 298 binding sites (Figure S7). We defined common binding sites between the two experiments as binding sites located within 500 bp, and identified 73 PRR7 binding sites. The binding sites determined by QUEST were compared with TAIR10 genes to associate binding sites with putative target genes. Genes were associated with binding sites located within 1000 bp upstream of the transcriptional start site to 1000 bp downstream of the transcriptional stop. Details are described in Appendix S7.

Identification of common DNA elements in regions close to PRR7 binding sites

Flanking sequences around each binding site were acquired using a publicly available script (http://www.stanford.edu/%7Evalouev/QuEST/output_genomic_regions_from_calls.pl.gz). Over-represented motifs were identified using MEME (Mustroph *et al.*, 2009) and WEEDER (Pavesi *et al.*, 2006). Significant motifs were defined as having an E-value <0.001. We used positional weight matrices (PWMs) to search for specific motifs of interest, including the G-BOX (CACGTG), ABA-responsive element (C/T)ACGTGGC, evening element (AAAATATCT), and CCA1 binding site AA(A/C)AATCT (Zou *et al.*, 2011). The mapping P-value was set at $<10^{-4}$, the mapping score threshold was set to 0.9, and the background AT and GC frequency was specified as 0.33 and 0.17, respectively. We looked for these elements in the promoter region (1000 bp upstream of the transcriptional start site) for 79 out of 113 genes that had a PRR7 binding site located in the upstream region, and compared them with genome-wide data. We specifically searched for the LUX binding site [GAT(A/T)CG], as a PWM had not been generated for this motif.

Comparison of PRR7 target genes and other data sets

The Fisher's exact test implemented in R (fisher.test) was used to determine the enrichment of PRR7 targets in different data sets. A functional analysis of PRR7 targets was performed using DAVID (Huang *et al.*, 2009b). Cycling gene expression was analyzed using PHASER (Michael *et al.*, 2008). Genes were defined as cycling if the model-based, pattern-matching algorithm > 0.8.

Determination of chlorophyll content

Chlorophylls were extracted from the 4-week-old seedlings with four seedlings per millilitre of 80% acetone in the dark (Mackinney, 1941). The chlorophyll contents were then measured using a spectrophotometer at wavelengths of 645 and 663 nm, with 80% acetone as a blank. Chlorophyll content was calculated as micrograms of chlorophyll per mg of fresh leaves using the following equation: chlorophyll $a + b$ (mg gFW^{-1}) = $(8.02 \times A_{663} + 20.20 \times A_{645}) \times (1/W)$; where W indicates the fresh weight of seedlings in milligrams.

Stomata conductance measurements

Stomata conductance was measured using an open infrared gas analysis system: LI-COR 6400. For all lines, fully expanded 7-week-old rosette leaves were used in a standard single-leaf chamber (chamber area = 6 cm²). An air mixture consisting of 20% O₂ and 80% N₂ was fed to the leaves, and the CO₂ levels were set to 400 ppm in the reference cell. The leaves were illuminated under a photosynthetic photon flux density (PPFD) of 400 µmol m⁻² sec⁻¹. Leaf temperature was held at 22–23°C, and the dew points within the chamber were kept at 14 ± 1.0°C. Before the start of each experiment, the leaves or the plants were acclimated to the conditions inside the chamber for at least 20 min under 400 µmol m⁻² sec⁻¹ of light. Measurements were carried out between ZT2 and ZT9.

Analysis of circadian rhythms

Ten-day-old seedlings growing on MS/0.8% agar/2% sucrose media with 12-h light/12-h dark at 22°C were transferred to a 96-well white plate with approximately 50 µl of the same media. A 20-µl volume of 5 mM luciferin in 0.01% silwett was added to each seedling. The plate was transferred the next day to constant light conditions and bioluminescence was detected using a Berthold LB960XS luminometer. For the ABA treatment, 30 µl of 25 µM ABA or methanol (diluent control) in 0.01% silwett was added to the seedlings at ZT29.

ACKNOWLEDGEMENTS

We thank K. Childs and other members of the Buell lab for help with data analysis, the Shiu lab for advice on the analysis of promoter elements and P. Salome, S. Matsubara and F. Gaymard for the provision of Arabidopsis lines. We are grateful to N. Bolduc and S. Hake, for the provision of an initial library preparation protocol, and the Howe and Thomashow labs for primers. We also thank S. Weise and T. Sharkey for help with the conductance measurements. We thank S. Hoffmann-Benning, B. Montgomery and S. Shiu for critically reading the article, and the MSU Research Technology Support Facility for sequencing. This work was supported by the National Science Foundation (IOS 1054243) and Michigan State University. T.L. was supported by the US Department of Energy and the Michigan Agricultural Experiment Station (DE-FG02-91ER20021).

SUPPORTING INFORMATION

Additional Supporting Information may be found in the online version of this article.

Figure S1. ChIP-Seq confirms the binding of PRR7 to the promoters of *CCA1* and *LHY*.

Figure S2. Expression of putative genes associated with PRR7 binding sites in wild type, PRR7 overexpressor, and the *prp579* triple mutant.

Figure S3. Motifs significantly enriched at PRR7 binding sites located upstream of a gene.

Figure S4. *TOC1* RNA levels in the presence or absence of exogenous ABA.

Figure S5. *CCA1* and *LHY* expression levels in *prp7,9 amiR* *CCA1* *LHY* lines.

Figure S6. Translatome data for *TOC1*, *PRR5*, *PRR7* and *PRR9*.

Figure S7. Schematic representation of sample comparisons for binding site identification using QUEST, and analysis of target genes identified in experiment I and/or experiment II.

Appendix S1. PRR7 binding site identification using ChIP-seq.

Appendix S2. PRR7 target genes indentified in other experiments.

Appendix S3. Primers used in this study.

Appendix S4. Chromatin Immunoprecipitation.

Appendix S5. Library preparation for sequencing.

Appendix S6. Confirmation of PRR7 binding by ChIP-qPCR.

Appendix S7. ChIP-Seq data analysis.

REFERENCES

- Bailey, T.L., Williams, N., Mistle, C. and Li, W.W. (2006) MEME: discovering and analyzing DNA and protein sequence motifs. *Nucleic Acids Res.* **34**, W369–W373.
- Bell-Pedersen, D., Cassone, V.M., Earnest, D.J., Golden, S.S., Hardin, P.E., Thomas, T.L. and Zoran, M.J. (2005) Circadian rhythms from multiple oscillators: lessons from diverse organisms. *Nat. Rev. Genet.* **6**, 544–556.
- Blasing, O.E., Gibon, Y., Gunther, M., Hohne, M., Morcuende, R., Osuna, D., Thimm, O., Usadel, B., Scheible, W.R. and Stitt, M. (2005) Sugars and circadian regulation make major contributions to the global regulation of diurnal gene expression in Arabidopsis. *Plant Cell*, **17**, 3257–3281.
- Briat, J.F., Ravet, K., Arnaud, N., Duc, C., Boucherez, J., Touraine, B., Cellier, F. and Gaymard, F. (2010) New insights into ferritin synthesis and function highlight a link between iron homeostasis and oxidative stress in plants. *Ann. Bot.* **105**, 811–822.
- Chattopadhyay, S., Ang, L.H., Puente, P., Deng, X.W. and Wei, N. (1998) Arabidopsis bZIP protein HY5 directly interacts with light-responsive promoters in mediating light control of gene expression. *Plant Cell*, **10**, 673–683.
- Chen, H., Zhang, J., Neff, M.M., Hong, S.W., Zhang, H., Deng, X.W. and Xiong, L. (2008) Integration of light and abscisic acid signaling during seed germination and early seedling development. *Proc. Natl Acad. Sci. USA*, **105**, 4495–4500.
- Covington, M.F., Maloof, J.N., Straume, M., Kay, S.A. and Harmer, S.L. (2008) Global transcriptome analysis reveals circadian regulation of key pathways in plant growth and development. *Genome Biol.* **9**, R130.
- Cutler, S.R., Rodriguez, P.L., Finkelstein, R.R. and Abrams, S.R. (2010) Abscisic acid: emergence of a core signaling network. *Annu. Rev. Plant Biol.* **61**, 651–679.
- Dixon, L.E., Knox, K., Kozma-Bognar, L., Southern, M.M., Pokhilko, A. and Millar, A.J. (2011) Temporal repression of core circadian genes is mediated through EARLY FLOWERING 3 in Arabidopsis. *Curr. Biol.* **21**, 120–125.
- Doherty, C.J. and Kay, S.A. (2010) Circadian control of global gene expression patterns. *Annu. Rev. Genet.* **44**, 419–444.
- Dong, M.A., Farre, E.M. and Thomashow, M.F. (2011) Circadian clock-associated 1 and late elongated hypocotyl regulate expression of the C-repeat binding factor (CBF) pathway in Arabidopsis. *Proc. Natl Acad. Sci. USA*, **108**, 7241–7246.
- Du, S.Y., Zhang, X.F., Lu, Z., Xin, Q., Wu, Z., Jiang, T., Lu, Y., Wang, X.F. and Zhang, D.P. (2012) Roles of the different components of magnesium chelatase in abscisic acid signal transduction. *Plant Mol. Biol.* **80**, 519–537.
- Edwards, K.D., Anderson, P.E., Hall, A., Salathia, N.S., Locke, J.C., Lynn, J.R., Straume, M., Smith, J.Q. and Millar, A.J. (2006) FLOWERING LOCUS C mediates natural variation in the high-temperature response of the Arabidopsis circadian clock. *Plant Cell*, **18**, 639–650.
- Farre, E.M. and Kay, S.A. (2007) PRR7 protein levels are regulated by light and the circadian clock in Arabidopsis. *Plant J.* **52**, 548–560.
- Farre, E.M., Harmer, S.L., Harmon, F.G., Yanovsky, M.J. and Kay, S.A. (2005) Overlapping and distinct roles of PRR7 and PRR9 in the Arabidopsis circadian clock. *Curr. Biol.* **15**, 47–54.
- Filichkin, S.A., Breton, G., Priest, H.D., Dharmawardhana, P., Jaiswal, P., Fox, S.E., Michael, T.P., Chory, J., Kay, S.A. and Mockler, T.C. (2011) Global profiling of rice and poplar transcriptomes highlights key conserved circadian-controlled pathways and cis-regulatory modules. *PLoS One*, **6**, e16907.
- Fowler, S. and Thomashow, M.F. (2002) Arabidopsis transcriptome profiling indicates that multiple regulatory pathways are activated during cold acclimation in addition to the CBF cold response pathway. *Plant Cell*, **14**, 1675–1690.
- Fukushima, A., Kusano, M., Nakamichi, N., Kobayashi, M., Hayashi, N., Sakakibara, H., Mizuno, T. and Saito, K. (2009) Impact of clock-associated

- Arabidopsis pseudo-response regulators in metabolic coordination. *Proc. Natl Acad. Sci. USA*, **106**, 7251–7256.
- Garcia, M.E., Lynch, T., Peeters, J., Snowden, C. and Finkelstein, R. (2008) A small plant-specific protein family of ABI five binding proteins (AFPs) regulates stress response in germinating Arabidopsis seeds and seedlings. *Plant Mol. Biol.* **67**, 643–658.
- Gendron, J.M., Pruneda-Paz, J.L., Doherty, C.J., Gross, A.M., Kang, S.E. and Kay, S.A. (2012) Arabidopsis circadian clock protein, TOC1, is a DNA-binding transcription factor. *Proc. Natl Acad. Sci. USA*, **109**, 3167–3172.
- Gilmour, S.J., Zarka, D.G., Stockinger, E.J., Salazar, M.P., Houghton, J.M. and Thomashow, M.F. (1998) Low temperature regulation of the Arabidopsis CBF family of AP2 transcriptional activators as an early step in cold-induced COR gene expression. *Plant J.* **16**, 433–442.
- Hanano, S., Domagalska, M.A., Nagy, F. and Davis, S.J. (2006) Multiple phytohormones influence distinct parameters of the plant circadian clock. *Genes Cells*, **11**, 1381–1392.
- Harmon, F.G. and Kay, S.A. (2003) The F box protein AFR is a positive regulator of phytochrome A-mediated light signaling. *Curr. Biol.* **13**, 2091–2096.
- Holm, M., Ma, L.G., Qu, L.J. and Deng, X.W. (2002) Two interacting bZIP proteins are direct targets of COP1-mediated control of light-dependent gene expression in Arabidopsis. *Genes Dev.* **16**, 1247–1259.
- Hsieh, T.H., Lee, J.T., Yang, P.T., Chiu, L.H., Charng, Y.Y., Wang, Y.C. and Chan, M.T. (2002) Heterology expression of the Arabidopsis C-repeat/dehydration response element binding factor 1 gene confers elevated tolerance to chilling and oxidative stresses in transgenic tomato. *Plant Physiol.* **129**, 1086–1094.
- Huang da, W., Sherman, B.T. and Lempicki, R.A. (2009a) Bioinformatics enrichment tools: paths toward the comprehensive functional analysis of large gene lists. *Nucleic Acids Res.* **37**, 1–13.
- Huang da, W., Sherman, B.T. and Lempicki, R.A. (2009b) Systematic and integrative analysis of large gene lists using DAVID bioinformatics resources. *Nat. Protoc.* **4**, 44–57.
- Huang, W., Perez-Garcia, P., Pokhilko, A., Millar, A.J., Antoshechkin, I., Riechmann, J.L. and Mas, P. (2012) Mapping the core of the Arabidopsis circadian clock defines the network structure of the oscillator. *Science*, **336**, 75–79.
- Hudson, M.E. and Quail, P.H. (2003) Identification of promoter motifs involved in the network of phytochrome A-regulated gene expression by combined analysis of genomic sequence and microarray data. *Plant Physiol.* **133**, 1605–1616.
- Indorf, M., Cordero, J., Neuhaus, G. and Rodríguez-Franco, M. (2007) Salt tolerance (STO), a stress-related protein, has a major role in light signaling. *Plant J.* **51**, 563–574.
- Jiao, Y., Lau, O.S. and Deng, X.W. (2007) Light-regulated transcriptional networks in higher plants. *Nat. Rev. Genet.* **8**, 217–230.
- Khan, S., Rowe, S.C. and Harmon, F.G. (2010) Coordination of the maize transcriptome by a conserved circadian clock. *BMC Plant Biol.* **10**, 126.
- Kidokoro, S., Maruyama, K., Nakashima, K. et al. (2009) The phytochrome-interacting factor PIF7 negatively regulates DREB1 expression under circadian control in Arabidopsis. *Plant Physiol.* **151**, 2046–2057.
- Kilian, J., Whitehead, D., Horak, J., Wanke, D., Weinl, S., Batistic, O., D'Angelo, C., Bornberg-Bauer, E., Kudla, J. and Harter, K. (2007) The AtGenExpress global stress expression data set: protocols, evaluation and model data analysis of UV-B light, drought and cold stress responses. *Plant J.* **50**, 347–363.
- Kinmonth-Schultz, H.A., Golembeski, G.S. and Imaizumi, T. (2013) Circadian clock-regulated physiological outputs: Dynamic responses in nature. *Semin. Cell Dev. Biol.* **5**, 407–413.
- Kumagai, T., Ito, S., Nakamichi, N., Niwa, Y., Murakami, M., Yamashino, T. and Mizuno, T. (2008) The common function of a novel subfamily of B-Box zinc finger proteins with reference to circadian-associated events in *Arabidopsis thaliana*. *Biosci. Biotechnol. Biochem.* **72**, 1539–1549.
- Kunihiro, A., Yamashino, T., Nakamichi, N., Niwa, Y., Nakanishi, H. and Mizuno, T. (2011) PHYTOCHROME-INTERACTING FACTOR 4 and 5 (PIF4 and PIF5) activate the homeobox ATHB2 and auxin-inducible IAA29 genes in the coincidence mechanism underlying photoperiodic control of plant growth of *Arabidopsis thaliana*. *Plant Cell Physiol.* **52**, 1315–1329.
- Kuno, N., Moller, S.G., Shinomura, T., Xu, X., Chua, N.H. and Furuya, M. (2003) The novel MYB protein EARLY-PHYTOCHROME-RESPONSIVE1 is a component of a slave circadian oscillator in Arabidopsis. *Plant Cell*, **15**, 2476–2488.
- Lai, A.G., Doherty, C.J., Mueller-Roeber, B., Kay, S.A., Schippers, J.H. and Dijkwel, P.P. (2012) CIRCADIAN CLOCK-ASSOCIATED 1 regulates ROS homeostasis and oxidative stress responses. *Proc. Natl Acad. Sci. USA*, **109**, 17129–17134.
- Langmead, B., Trapnell, C., Pop, M. and Salzberg, S.L. (2009) Ultrafast and memory-efficient alignment of short DNA sequences to the human genome. *Genome Biol.* **10**, R25.
- Lee, J., He, K., Stolt, V., Lee, H., Figueroa, P., Gao, Y., Tongprasit, W., Zhao, H., Lee, I. and Deng, X.W. (2007) Analysis of transcription factor HY5 genomic binding sites revealed its hierarchical role in light regulation of development. *Plant Cell*, **19**, 731–749.
- Legnaioli, T., Cuevas, J. and Mas, P. (2009) TOC1 functions as a molecular switch connecting the circadian clock with plant responses to drought. *EMBO J.* **28**, 3745–3757.
- Mackinney, G. (1941) Absorption of light by chlorophyll solutions. *J. Biol. Chem.* **140**, 315–322.
- McClung, C.R. (2011) The genetics of plant clocks. *Adv. Genet.* **74**, 105–139.
- Michael, T.P., Mockler, T.C., Breton, G. et al. (2008) Network discovery pipeline elucidates conserved time-of-day-specific cis-regulatory modules. *PLoS Genet.* **4**, e14.
- Mizoguchi, T., Wheatley, K., Hanzawa, Y., Wright, L., Mizoguchi, M., Song, H.R., Carre, I.A. and Coupland, G. (2002) LHY and CCA1 are partially redundant genes required to maintain circadian rhythms in Arabidopsis. *Dev. Cell*, **2**, 629–641.
- Murashige, T. and Skoog, F. (1962) A revised medium for rapid growth and bio assays with tobacco tissue cultures. *Physiol. Plant.* **15**, 473–497.
- Mustroph, A., Zanetti, M.E., Jang, C.J., Holtan, H.E., Repetti, P.P., Galbraith, D.W., Girke, T. and Bailey-Serres, J. (2009) Profiling translomes of discrete cell populations resolves altered cellular priorities during hypoxia in Arabidopsis. *Proc. Natl Acad. Sci. USA*, **106**, 18843–18848.
- Nakamichi, N. (2011) Molecular mechanisms underlying the Arabidopsis circadian clock. *Plant Cell Physiol.* **52**, 1709–1718.
- Nakamichi, N., Kita, M., Ito, S., Yamashino, T. and Mizuno, T. (2005) PSEUDO-RESPONSE REGULATORS, PRR9, PRR7 and PRR5, together play essential roles close to the circadian clock of *Arabidopsis thaliana*. *Plant Cell Physiol.* **46**, 686–698.
- Nakamichi, N., Kita, M., Niinuma, K., Ito, S., Yamashino, T., Mizoguchi, T. and Mizuno, T. (2007) Arabidopsis clock-associated pseudo-response regulators PRR9, PRR7 and PRR5 coordinately and positively regulate flowering time through the canonical CONSTANS-dependent photoperiodic pathway. *Plant Cell Physiol.* **48**, 822–832.
- Nakamichi, N., Kusano, M., Fukushima, A., Kita, M., Ito, S., Yamashino, T., Saito, K., Sakakibara, H. and Mizuno, T. (2009) Transcript profiling of an Arabidopsis PSEUDO RESPONSE REGULATOR arrhythmic triple mutant reveals a role for the circadian clock in cold stress response. *Plant Cell Physiol.* **50**, 447–462.
- Nakamichi, N., Kiba, T., Henriques, R., Mizuno, T., Chua, N.H. and Sakakibara, H. (2010) PSEUDO-RESPONSE REGULATORS 9, 7, and 5 are transcriptional repressors in the Arabidopsis circadian clock. *Plant Cell*, **22**, 594–605.
- Nakamichi, N., Kiba, T., Kamioka, M., Suzuki, T., Yamashino, T., Higashiyama, T., Sakakibara, H. and Mizuno, T. (2012) Transcriptional repressor PRR5 directly regulates clock-output pathways. *Proc. Natl Acad. Sci. USA*, **109**, 17123–17128.
- Nemhauser, J.L., Hong, F. and Chory, J. (2006) Different plant hormones regulate similar processes through largely nonoverlapping transcriptional responses. *Cell*, **126**, 467–475.
- Niyogi, K.K., Grossman, A.R. and Bjorkman, O. (1998) Arabidopsis mutants define a central role for the xanthophyll cycle in the regulation of photosynthetic energy conversion. *Plant Cell*, **10**, 1121–1134.
- Nozue, K., Covington, M.F., Duek, P.D., Lorrain, S., Fankhauser, C., Harmer, S.L. and Maloof, J.N. (2007) Rhythmic growth explained by coincidence between internal and external cues. *Nature*, **448**, 358–361.
- Nozue, K., Harmer, S.L. and Maloof, J.N. (2011) Genomic analysis of circadian clock-, light-, and growth-correlated genes reveals PHYTOCHROME-INTERACTING FACTOR5 as a modulator of auxin signaling in Arabidopsis. *Plant Physiol.* **156**, 357–372.
- Nusinow, D.A., Helfer, A., Hamilton, E.E., King, J.J., Imaizumi, T., Schultz, T.F., Farre, E.M. and Kay, S.A. (2011) The ELF4-ELF3-LUX complex links

- the circadian clock to diurnal control of hypocotyl growth. *Nature*, **475**, 398–402.
- Oh, E., Kang, H., Yamaguchi, S., Park, J., Lee, D., Kamiya, Y. and Choi, G. (2009) Genome-wide analysis of genes targeted by PHYTOCHROME INTERACTING FACTOR 3-LIKE5 during seed germination in Arabidopsis. *Plant Cell*, **21**, 403–419.
- Ouyang, X., Li, J., Li, G. *et al.* (2011) Genome-wide binding site analysis of FAR-RED ELONGATED HYPOCOTYL3 reveals its novel function in Arabidopsis development. *Plant Cell*, **23**, 2514–2535.
- Pavesi, G., Mereghetti, P., Mauri, G. and Pesole, G. (2004) Weeder Web: discovery of transcription factor binding sites in a set of sequences from co-regulated genes. *Nucleic Acids Res.* **32**, W199–W203.
- Pavesi, G., Mereghetti, P., Zambelli, F., Stefani, M., Mauri, G. and Pesole, G. (2006) MoD Tools: regulatory motif discovery in nucleotide sequences from co-regulated or homologous genes. *Nucleic Acids Res.* **34**, W566–W570.
- Pokhilko, A., Fernandez, A.P., Edwards, K.D., Southern, M.M., Halliday, K.J. and Millar, A.J. (2012) The clock gene circuit in Arabidopsis includes a repressilator with additional feedback loops. *Mol. Syst. Biol.* **8**, 574.
- Pruneda-Paz, J.L., Breton, G., Para, A. and Kay, S.A. (2009) A functional genomics approach reveals CHE as a component of the Arabidopsis circadian clock. *Science*, **323**, 1481–1485.
- Ravet, K., Touraine, B., Boucherez, J., Briat, J.F., Gaymard, F. and Cellier, F. (2009) Ferritins control interaction between iron homeostasis and oxidative stress in Arabidopsis. *Plant J.* **57**, 400–412.
- Rawat, R., Schwartz, J., Jones, M.A., Sairanen, I., Cheng, Y., Andersson, C.R., Zhao, Y., Ljung, K. and Harmer, S.L. (2009) REVEILLE1, a Myb-like transcription factor, integrates the circadian clock and auxin pathways. *Proc. Natl Acad. Sci. USA*, **106**, 16883–16888.
- Rey, G., Cesbron, F., Rougemont, J., Reinke, H., Brunner, M. and Naef, F. (2011) Genome-wide and phase-specific DNA-binding rhythms of BMAL1 control circadian output functions in mouse liver. *PLoS Biol.* **9**, e1000595.
- Salome, P.A. and McClung, C.R. (2005) PSEUDO-RESPONSE REGULATOR 7 and 9 are partially redundant genes essential for the temperature responsiveness of the Arabidopsis circadian clock. *Plant Cell*, **17**, 791–803.
- Sawa, M., Nusinow, D.A., Kay, S.A. and Imaizumi, T. (2007) FKF1 and GIGANTEA complex formation is required for day-length measurement in Arabidopsis. *Science*, **318**, 261–265.
- Song, Y.H., Ito, S. and Imaizumi, T. (2011) Similarities in the circadian clock and photoperiodism in plants. *Curr. Opin. Plant Biol.* **13**, 594–603.
- Strayer, C., Oyama, T., Schultz, T.F., Raman, R., Somers, D.E., Mas, P., Panda, S., Kreps, J.A. and Kay, S.A. (2000) Cloning of the Arabidopsis clock gene TOC1, an autoregulatory response regulator homolog. *Science*, **289**, 768–771.
- Valouev, A., Johnson, D.S., Sundquist, A., Medina, C., Anton, E., Batzoglou, S., Myers, R.M. and Sidow, A. (2008) Genome-wide analysis of transcription factor binding sites based on ChIP-Seq data. *Nat. Methods*, **5**, 829–834.
- Wang, Z.Y. and Tobin, E.M. (1998) Constitutive expression of the CIRCADIAN CLOCK ASSOCIATED 1 (CCA1) gene disrupts circadian rhythms and suppresses its own expression. *Cell*, **93**, 1207–1217.
- Wang, L., Kim, J. and Somers, D.E. (2013) Transcriptional corepressor TOPLESS complexes with pseudoresponse regulator proteins and histone deacetylases to regulate circadian transcription. *Proc. Natl Acad. Sci. USA*, **110**, 761–766.
- Wenkel, S., Turck, F., Singer, K., Gissot, L., Le Gourrierec, J., Samach, A. and Coupland, G. (2006) CONSTANS and the CCAAT box binding complex share a functionally important domain and interact to regulate flowering of Arabidopsis. *Plant Cell*, **18**, 2971–2984.
- Xiong, L., Lee, H., Ishitani, M. and Zhu, J.K. (2002) Regulation of osmotic stress-responsive gene expression by the LOS6/ABA1 locus in Arabidopsis. *J. Biol. Chem.* **277**, 8588–8596.
- Yadav, V., Mallappa, C., Gangappa, S.N., Bhatia, S. and Chattopadhyay, S. (2005) A basic helix-loop-helix transcription factor in Arabidopsis, MYC2, acts as a repressor of blue light-mediated photomorphogenic growth. *Plant Cell*, **17**, 1953–1966.
- Yamashino, T., Matsushika, A., Fujimori, T., Sato, S., Kato, T., Tabata, S. and Mizuno, T. (2003) A Link between circadian-controlled bHLH factors and the APRR1/TOC1 quintet in *Arabidopsis thaliana*. *Plant Cell Physiol.* **44**, 619–629.
- Zhang, X., Chen, Y., Wang, Z.Y., Chen, Z., Gu, H. and Qu, L.J. (2007) Constitutive expression of CIR1 (RVE2) affects several circadian-regulated processes and seed germination in Arabidopsis. *Plant J.* **51**, 512–525.
- Zou, C., Sun, K., Mackaluso, J.D., Seddon, A.E., Jin, R., Thomashow, M.F. and Shiu, S.H. (2011) Cis-regulatory code of stress-responsive transcription in *Arabidopsis thaliana*. *Proc. Natl Acad. Sci. USA*, **108**, 14992–14997.